

## Particle-in-cell simulations of Langmuir probes at COMPASS tokamak

A. Podolník<sup>1,2</sup>, M. Komm<sup>1</sup>, J. Adámek<sup>1</sup>, P. Háček<sup>1,2</sup>, J. Krbec<sup>1,3</sup>, R. Dejarnac<sup>1</sup>,

R. Pánek<sup>1</sup>, J. P. Gunn<sup>4</sup> and the COMPASS Team

<sup>1</sup> Institute of Plasma Physics of the CAS, Prague, Czech Republic

<sup>2</sup> Faculty of Mathematics and Physics, Charles University, Prague, Czech Republic

<sup>3</sup> FNSPE, Czech Technical University in Prague, Prague, Czech Republic

<sup>4</sup> CEA, IRFM, F-13108 Saint Paul Lez Durance, France

### Introduction

Langmuir probes are amongst the most versatile tools for plasma diagnostics for both magnetized and unmagnetized plasmas. Analysis of  $I$ - $V$  characteristics measured by the probe can in principle yield values of electron temperature  $T_e$ , floating potential  $V_{fl}$  and electron density  $n_e$  as well as electron energy distribution function. However, correct values of these quantities can be determined only when all the instrumental effects on measured data are addressed. For magnetized plasma in the scrape-off layer of tokamak discharges, the prevalent influence is the sheath expansion due to presence of strong magnetic field. This effect is taken into account by introduction of fourth parameter to fit of the  $I$ - $V$  curve [1].

$$I_{pin} = I_{sat} \left( 1 - \exp \left( -\frac{V - V_{fl}}{T_e} \right) \right) - R(V - V_{fl}) \quad (1)$$

To determine density from the measurement, one should know the size of the ion collecting area. For unmagnetized plasmas with high Debye shielding, simple model can be used and the area is usually identified with the probe surface exposed to the plasma. Magnetic field introduces the Larmor rotation which requires a more sophisticated approach. Modelling of ion collection by the probe can be employed to determine the collecting area in particular conditions for a real device, such as the COMPASS tokamak [2].

### Model and simulated conditions

A 3D3V particle-in-cell model SPICE3 [3] was used for the simulation of plasma conditions relevant to the COMPASS tokamak. The model itself is an extension of 2D model SPICE2 [4] and both of them have been successfully used to simulate advanced probes such as the ball-pen probe [5], plasma interaction with solid material at crossings of toroidal and

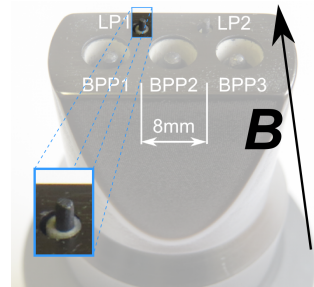


Figure 1: Langmuir probe pin (cutout) and its location on the probe head of reciprocating manipulator at COMPASS [2]. The dimensions of the pin are  $r = 0.45$  mm,  $h = 1.5$  mm.

poloidal divertor tile gaps [6] or heat loads on leading edges under ITER-relevant conditions [7].

The simulated probe geometry matches the dimensions of Langmuir probe pin used at the horizontal reciprocating manipulator (HRCP), which is located at the outer midplane of the COMPASS tokamak [2]. The pin has a form of a cylindrical carbon electrode with radius  $r_{\text{pin}} = 0.45$  mm and height  $h_{\text{pin}} = 1.5$  mm (Fig. 1) positioned on a probe head (a free floating block in the simulation). The model uses two injection/sink planes perpendicular to magnetic field, while other sides of the simulation box are periodic.

Following conditions were simulated. Magnetic field magnitude was kept constant at  $B = 1$  T and the ratio of ion to electron temperature  $T_i/T_e$  was  $\tau = 2$ , plasma density at injection plane varied in range  $n_0 = \langle 0.5, 2.0 \rangle \times 10^{18} \text{ m}^{-3}$  and electron temperature varied in range  $T_e = \langle 5, 50 \rangle \text{ eV}$ . During the simulation, the pin was swept by step-wise adjustment of its potential from  $-10 k_B T_e/e$  to  $10 k_B T_e/e$ , while the probe head was kept at floating potential (assumed as  $3 k_B T_e/e$  below plasma potential). Dimensions of the object simulating the probe head had a fixed ratio to  $r_L$  at 3.5.

## Data evaluation

Each simulation yielded an  $I$ - $V$  characteristic which was fitted using the standard 4-parametric fit (1). The density at sheath entrance could be determined from the ion saturation current using the relation  $I_{\text{sat}} = eA_{\text{eff}}n_{\text{SE}}c_s$ , while  $c_s = \sqrt{\frac{k_B(T_i+T_e)}{m_i}}$  being the sound velocity. As suggested in the introduction, the size of collecting area  $A_{\text{eff}}$  is unknown. We will relate the size of the area to the probe cross section ( $A_{\odot}$ ) in plane perpendicular to magnetic field vector using the effective area ratio coefficient  $q_A$  as  $A_{\text{eff}} = q_A A_{\odot}$ . For a fitted ion saturation current from eq. (1), we obtain the relation for  $q_A$ :

$$q_A|_{\text{simulated}} = \frac{I_{\text{sat}}}{e n_{\text{SE}} A_{\odot} \sqrt{\frac{k_B(T_i+T_e)}{m_i}}}. \quad (2)$$

There is only one unknown variable, the sheath entry density  $n_{\text{SE}}$ , since it is affected by the probe head. However, it can be evaluated from the simulation of unperturbed plasma on the other side of the free floating block, since all disturbances caused by swept pin potential are shielded on scale  $< r_L$  in direction perpendicular to magnetic field.

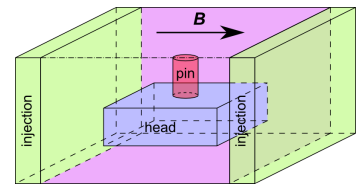


Figure 2: Simplified geometry of the model. A free floating object substituting the probe head is submerged to the plasma between two injection planes.

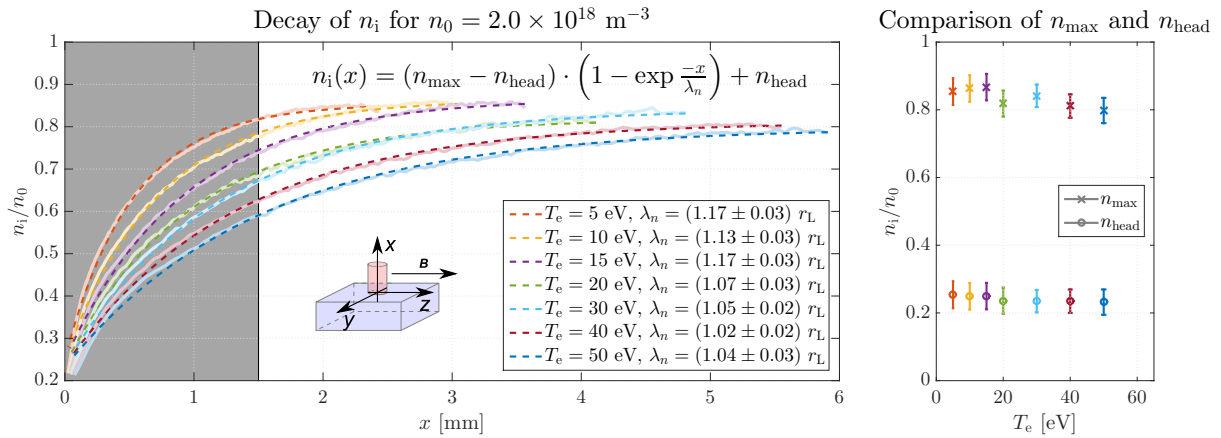


Figure 3: Density attenuation on the pin axis. The schema shows the location of the axis. The grey rectangle on the left represents the extent of the probe pin. The exponential decay is observed and fitted with the decay formula. The decay length  $\lambda_n \approx r_L$  is observed. Right panel compares maximal densities reached on the pin axis far from the pin. All  $n_{\max} \approx 0.8 \times n_0$ , which shows consistency of the model behavior, however, the density is affected by periodic repetition of the probe head in simulation space.

### Simulation results

First, the study of the density profile in the vicinity of probe head was performed. The region on the opposite side of the free floating block represents an unperturbed plasma near an object at  $V_{\text{fl}}$ . If the object is an infinite plane, the density in the magnetic pre-sheath can be approximated as an exponential decay with decay length equal to Larmor radius  $r_L$ :  $n_i(x) \approx n_0 \left(1 - \exp \frac{-x}{r_L}\right)$ . In the simulated cases, however, the object representing the probe head is still comparable to  $r_L$  and thus the density at  $x = 0$  is not zero. Therefore for the analysis of the simulations, the following modification of the decay formula is used:

$$n_i(x) = (n_{\max} - n_{\text{head}}) \left(1 - \exp \frac{-x}{r_L}\right) + n_{\text{head}}. \quad (3)$$

Quantities  $n_{\text{head}}$  and  $n_{\max}$  describe the finite size of the probe head as well as its influence on density distribution due to spatial repetition due to periodic boundary conditions. Value of  $n_{\max} \rightarrow n_0$  for infinite simulation box and  $n_{\text{head}} \rightarrow 0$  for infinite plane as probe head. The Fig. 3 illustrates decay of  $n_i$  for  $n_0 = 2.0 \times 10^{18} \text{ m}^{-3}$ . Values of  $n_{\text{head}}$  and  $n_{\max}$  were evaluated for each simulation. Finally, the attenuation of total flux to the probe can be addressed when the value of  $n_{\text{SE}}$  in the formula (2) is expressed as  $n_{\text{SE}} = \frac{1}{h_{\text{pin}}} \cdot \int_0^{h_{\text{pin}}} (n_{\max} - n_{\text{head}}) \left(1 - \exp \frac{-x}{r_L}\right) + n_{\text{head}} dx$ . Analytical expression of the integral and numerically integrated raw data differ by < 5 %.

Results of  $q_A$  evaluation are shown at Fig. 4. All simulated densities show similar behavior of  $q_A$  temperature (or  $r_L$ ) dependency which can be expressed as

$$q_A|_{\text{derived}}(r_L) = \frac{A_{\text{ext}}(r_L)}{A_{\odot}} \left[ q_{\text{head}} + q_{\max} \left(1 - \frac{r_L}{h_{\text{pin}}} \left(1 - \exp \frac{-h_{\text{pin}}}{r_L}\right)\right) \right]. \quad (4)$$

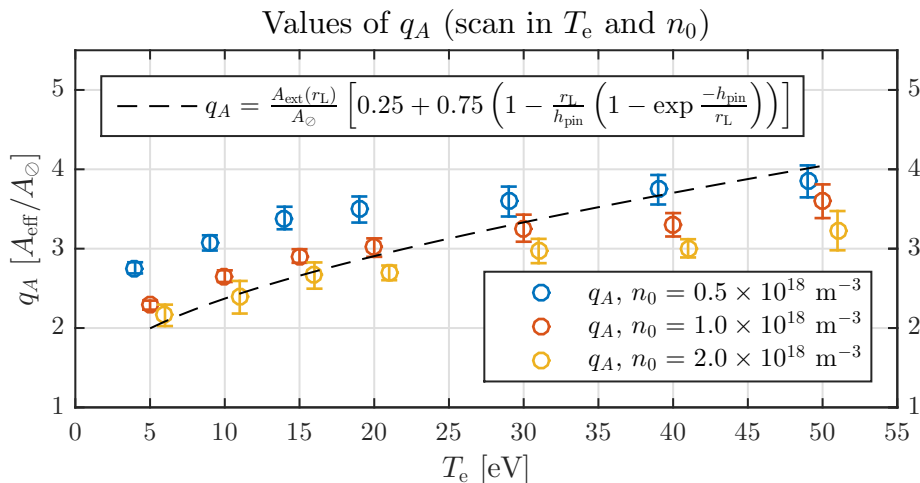


Figure 4: *Effective area ratio results. Values of  $q_A$  can be described by a formula (4) (dashed line) which takes into account both density attenuation and spreading of the collective area with Larmor radius. Ion temperature is defined as  $2T_e$  in all simulations.  $T_e$  is shifted by 1 eV for clarity.*

Where  $q_{\text{head}} = 0.25$  and  $q_{\text{max}} = 0.75$  were evaluated from the simulation (see Fig. 3). First term of the equation describes the broadening of the probe cross section with Larmor radius, since  $A_{\text{ext}}$  is defined as its extension by  $r_L$  as  $A_{\text{ext}} = A_{\odot} + 2h_{\text{pin}}r_L + 2r_{\text{pin}}r_L + \frac{1}{2}\pi r_L^2$ , because Larmor gyration allows collection of ions farther from the probe. The second term is an analytical expression of integral of the density attenuation (3) as it was observed in the simulation. For precise calculation of  $r_L$  the ratio of temperatures  $\tau$  should be known or assumed.

## Conclusions

It has been shown by the simulation that the Langmuir probe pin from HRCP at the COMPASS tokamak collects current from larger area than its cross section. The size of the area shows only slight dependency on plasma density and can be derived from known geometrical properties of the probe and  $T_e$  with assumed  $\tau$ . This relation can be expressed as formula (4).

## Acknowledgements

This work was supported by The Ministry of Education, Youth and Sports from the Large Infrastructures for Research, Experimental Development and Innovations project *IT4Innovations National Supercomputing Center – LM2015070* and also by the Czech Science Foundation project GA16-14228S. This research has been co-funded by MEYS projects number 8D15001 and LM2015045.

## References

- [1] J. P. Gunn et al., *Review of Scientific Instruments* **66**, 15 (1995)
- [2] J. Adamek et al., *Contributions to Plasma Physics* **279**, 3 (2014)
- [3] M. Komm et al., *Plasma Physics and Controlled Fusion* **55**, 025006 (2013)
- [4] R. Dejarnac et al., *Journal of Nuclear Materials* **390–391**, 818 (2008)
- [5] M. Komm et al., *Contributions to Plasma Physics* **50**, 9 (2010)
- [6] M. Komm et al., *Plasma Physics and Controlled Fusion* **53**, 115004 (2011)
- [7] R. A. Pitts et al., *Nuclear Materials and Energy* (2017), <https://doi.org/10.1016/j.nme.2017.03.005>